MERIT Self-directed Joint Research

Observation of superconductivity and investigation of its origin in monolayer graphene intercalation compounds

Haruko Toyama[1], Kentaro Horii[2]

[1]Hasegawa Laboratory, Department of Physics, The university of Tokyo
[2]Hirahara Laboratory, Department of Physics, Tokyo Institute of Technology

1. Authors

Haruko Toyama: Her specialized field is the study of the superconducting properties in two-dimensional structures grown on semiconductor substrates. In this study, Haruko Toyama made graphene intercalation compounds in ultrahigh vacuum (UHV) and performed *in-situ* four point probe transport measurements.

Kentaro Horii: His specialized study field is the control of the physical properties by intercalation of metal atoms. In this study, Kentaro Horii made graphene intercalation compounds in UHV and observed electronic structures by Angle-resolved photoemission spectroscopy (ARPES).

2. Background

Graphene, a two-dimensional material of carbon atoms with a honeycomb structure, is characterized by a linear band dispersion called the Dirac cone. It has attracted much attention in recent years due to its interesting properties, such as the half-integer quantum Hall effect, weak anti-localization, and high electron mobility. As with graphite, it is possible to intercalate atoms and molecules between the two to several layers of graphene, and these are called graphene intercalation compounds and are being studied intensively. Intercalation significantly changes the physical properties of graphene, and superconductivity has been shown to occur in Ca-intercalated graphene.

Ca-intercalated bilayer graphene on SiC substrates has been reported to reach zero resistance below ~2 K by *in-situ* transport measurements in UHV [1]. It is proposed in a previous report using ARPES measurements that the superconductivity in Ca-intercalated bilayer graphene is attributed to the interlayer band (ILB), which is a hybridization of the electronic states of Ca atoms and the free-electron like band in the unoccupied state of graphene [2]. There are other candidates for the origin of the superconductivity in graphene interlayers. For example, in Li-intercalated graphene, ARPES

measurements suggest that the superconductivity is due to the π* band having strong electron-lattice interactions with phonon [3]. In recent years, the van Hove singularity (vHs), a flat dispersion near the $\bar{M}$ point, has also attracted much attention because theoretical calculations predicted vHs-derived topological superconductivity with non-zero topological invariants [4]. The flat bands of vHs are usually located about 2 eV away from the Fermi level in the unoccupied and occupied states of pristine graphene and thus are unlikely to contribute to the transport. However, it has been reported that the Fermi level can be tuned to vHs by electron doping in monolayer graphene on SiC by Ca intercalation and by modification of the surface with Ca and K atoms [5], raising the possibility of topological superconductivity in graphene.

For Ca-intercalated bilayer graphene, a stacking model in which Ca atoms are intercalated between bilayer graphene layers was assumed and ILBs were thought to contribute to superconductivity as an analogy to superconducting Ca-intercalated graphite compound in a previous study [2], but the results were still inconclusive. Endo et al. attempted to clarify a more accurate stacking model using total reflection high energy positron diffraction, and found that Ca atoms are placed underneath the bilayer graphene layers, rather than between bilayer graphene layers as previously thought [6]. In the case of graphene on SiC substrates, there is a layer of carbon atoms bonded to the substrate (called buffer layer) between the SiC substrate and the freestanding bilayer graphene, which means that Ca atoms are intercalated between the lower layer of bilayer graphene and the buffer layer. Following this model, Endo performed Ca intercalation and transport measurements on a monolayer sample (monolayer freestanding graphene with a buffer layer beneath it), and observed the superconducting transition in the monolayer graphene as in the bilayer sample [7].

Therefore, it is necessary to discuss the mechanism of superconductivity in Ca-intercalated graphene in more detail, including the possible contribution of vHs and π* bands, which remain to be verified, based on an accurate stacking model including the buffer layer and substrate SiC. For this purpose, a systematic investigation of the surface structure, electronic structure, and transport properties is required, which has not been done so far.

3. Purpose

In this study, we clarify the mechanism of superconductivity in superconducting graphene intercalation compounds through a systematic investigation using both transport and ARPES measurement approaches.

4. Method

In this study, all the methods are performed under ultrahigh vacuum (UHV), which enables us to measure the intrinsic properties without the possibility of sample degradation or structural change due

to atmospheric exposure.

4.1. Transport measurements

The transport properties were measured using an *in-situ* four-point transport measurement system installed in Hasegawa Laboratory. The lowest attainable temperature of the sample is ~0.8 K and the magnetic field can be applied up to 7 T in the direction perpendicular to the sample surface.

4.2. ARPES measurements

The electronic structure was observed using the ARPES measurement system installed in Hirahara Laboratory. Measurements were performed at room temperature using an excitation energy of HeIα (21.2 eV) in a He discharge lamp. The energy analyzer for photoelectron spectroscopy was a ScientaOmicron R4000.

5. Sample fabrication

5.1. Fabrication of monolayer graphene on SiC substrates

Monolayer graphene was grown on SiC substrates by degassing the SiC substrates at ~600 °C in a vacuum chamber and then heating them at ~1620 °C for 20 min in an Ar gas atmosphere at atmospheric pressure. This fabrication method is called the thermal decomposition method [8]. This method yields a sample of fully freestanding monolayer graphene on a SiC substrate via a buffer layer (an insulating carbon monatomic layer bonded to the substrate). Although epitaxial graphene grown by thermal decomposition method is known to be difficult to fabricate to the targeted number of layers, the graphene sample fabricated in this study has a dominant monolayer and some regions of bilayer, as confirmed by ARPES measurements and Raman spectroscopy. In addition, the Raman spectroscopy results show that the graphene sample has few defects.

5.2. Fabrication of Li- and Ca-intercalated graphene

The fabricated monolayer graphene on SiC was introduced into the UHV chamber for sample preparation, degassed, and then intercalated samples were prepared. In the RHEED pattern of pristine graphene (Fig. 1 (a)), diffraction spots originating from the SiC substrate, graphene, and buffer layer were observed. When Li was deposited on the monolayer graphene at room temperature by molecular beam epitaxy method, the RHEED pattern shows that the spots with $6\sqrt{3}\times6\sqrt{3}$-R30º periodicity originating from the buffer layer first weakened (Fig. 1 (b)), suggesting that the bond between the buffer layer and the SiC substrate was broken by Li deposition. In other words, Li terminated on the SiC substrate surface, and freestanding bilayer graphene was formed. After further Li deposition, a pattern with $\sqrt{3}\times\sqrt{3}$-R30º periodicity appeared as shown in Fig. 1 (c), indicating that Li-intercalated graphene was fabricated.

Next, Ca was deposited on the Li-intercalated graphene while the temperature was maintained at

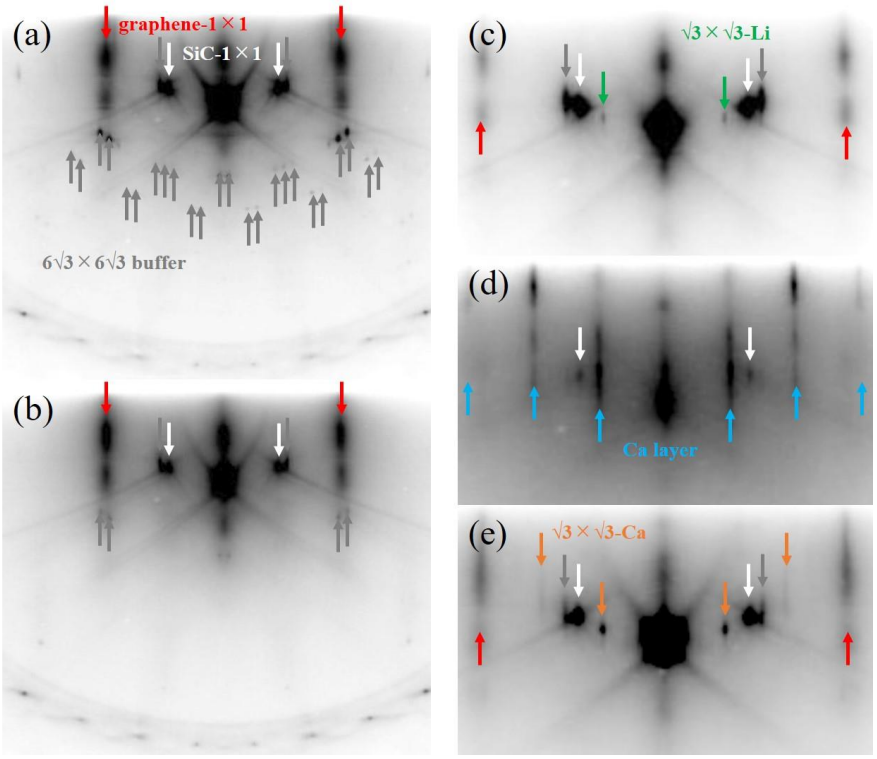

Figure 1, RHEED patterns of the sample preparation process. (a) pristine monolayer graphene, (b) Li-deposited sample, (c) Li-deposited sample on top of (b), (d) Ca-deposited sample on Li-intercalated graphene, (e) Ca-deposited sample followed by annealing. The spots originating from SiC-1×1 (white), graphene-1×1 (red), buffer layer 6√3×6√3-R30º (gray), Li-intercalated √3×√3 (green), Ca-layer (light blue), and Ca-intercalated √3×√3-R30º (orange) are indicated by arrows, respectively. Since there are many spots in the buffer layer 6√3×6√3-R30º, only a few representative spots are shown with arrows.

~200-270 °C to prevent the intercalated Li from desorbing, and as shown in Figure 1 (d), a new streak appeared that was different from the √3×√3-R30º of Li, indicating that a Ca layer grew on the top surface. When the sample was annealed at a high temperature of ~310 °C, the streak originating from the Ca layer disappeared and a spot with a period of √3×√3-R30º due to Ca intercalation appeared to replace it (Fig. 1 (e)). This suggests that the Ca atoms, which were only stacked on the top surface before annealing, were intercalated into the graphene layers by annealing. It was also shown that small clusters of excess Ca atoms still exist after annealing.

6. Results

6.1. Transport properties

Figure 2 (a) shows the results of transport measurements at each step of the sample preparation

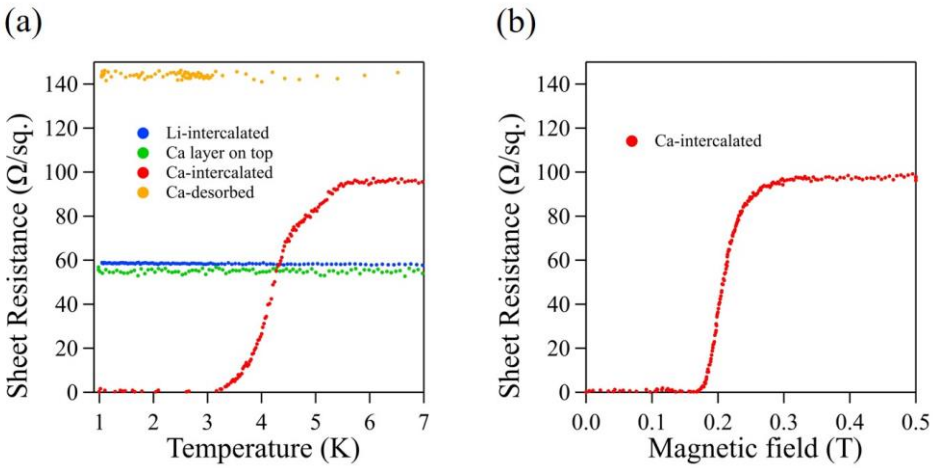

Figure 2, (a) temperature dependence and (b) magnetic field dependence of the sheet resistance determined by *in-situ* 4-point-probe transport measurements.

process. First of all, Li-intercalated graphene shows almost constant resistance at low temperatures below ~7 K, which can be described as metallic conduction. More precisely, the resistivity increases by about 2-3 % with decreasing temperature, which may be localization by surface defects generated during the fabrication process. Next, when the Ca layer was stacked on top of the Li-intercalated graphene, the resistance decreased due to electron doping from the deposited Ca, but the metallic behavior itself did not change.

However, when the Ca atoms were intercalated by annealing, the transport properties changed dramatically and a superconducting transition was observed. The superconducting transition temperature of Ca-intercalated graphene was found to be 5.7 K for T_{onset}, where the resistance begins to decrease, and 3.0 K for T_{zero}, where the resistance drops to zero. The difference between T_{onset} and T_{zero} is 2.7 K, which is much larger than that of other superconductors, i.e., it is a gentle transition, which cannot be fitted by the typical theoretical formula for two-dimensional superconductivity [9,10], but this trend is consistent with previous studies. In addition, the slope change is discontinuous at ~4.5 K, suggesting that the material has at least two transition temperatures, 5.7 K and 4.5 K. The discontinuous slope itself was also reproduced in another sample obtained by the same fabrication method, although the transition temperatures were different. The origin of the discontinuous slope may be due to the existence of multiple superconducting origins with different transition temperatures (e.g., a mixture of π* band and ILB superconductivity), or due to the inhomogeneity of the sample surface structure.

In order to further confirm that the observed phenomenon is superconductivity, we measured the magnetic field dependence and the results are shown in Fig. 2 (b). As a result of fitting analysis using the Ginzburg-Landau (GL) theory [11], the upper critical field and the GL coherence length are

determined to be H_{c2} = 0.27 T and ξ_{GL} = 35.2 nm, respectively. Note that the quantitative accuracy of H_{c2} and ξ_{GL} obtained from the GL theory must be carefully considered because, as mentioned above, the superconductivity in Ca-intercalated graphene cannot be explained by a simple two-dimensional superconducting model.

When the superconducting Ca-intercalated graphene was further annealed at high temperature until the √3×√3-R30º periodic spot disappeared, i.e., the intercalated Ca atoms were desorbed from the graphene, the superconductivity disappeared. These results indicate that superconductivity is induced in Ca-intercalated graphene.

6.2. Electronic structures

ARPES measurements were also carried out at each step of the sample preparation process as in the transport measurements. Focusing on the Dirac cone near the $\bar{K}$ point, we observed a change in the Dirac cone from a single Dirac cone due to the monolayer of pristine graphene before deposition to a double Dirac cone after Li deposition. Therefore, it can be also inferred from the electronic structure that the bond between the buffer layer and the SiC substrate was broken by Li deposition, resulting in the formation of freestanding bilayer graphene. The Dirac cone of Li-intercalated graphene is shifted downward by ~0.9 eV in the energy direction compared to that of pristine graphene, indicating that the deposited Li atoms doped electrons into the graphene. On the other hand, the valence band of bulk SiC near the $\bar{\Gamma}$ point also shifted in energy, and its apex was observed to be located ~0.6 eV below the Fermi level after Li intercalation, which may reflect the termination of bonds in the SiC substrate by Li atoms. Near the $\bar{M}$ point, the flat band of vHs is located within a few 10 meV from the Fermi level when Li-intercalated, suggesting that vHs may contribute to conduction. It was also found that the approximate shape of the electronic structure is almost unchanged by the stacking of Ca layers, which explains why the transport properties do not change much from Li-intercalated graphene when Ca is only stacked on the top surface.

When Ca was intercalated, the electronic structure changed. The Dirac cone near the $\bar{K}$ point became more electron-doped and shifted to a lower energy of ~0.3-0.4 eV than in the case of Li. The flat band near the $\bar{M}$ point also shifted to lower energy and consequently away from the Fermi level, making it unlikely that vHs contributes to the transport. On the other hand, the valence band of bulk SiC near the $\bar{\Gamma}$ point was similar to that of Li-intercalated graphene. This means that even in the Ca-intercalated graphene, the bulk SiC is considered to be terminated with Li atoms.

For ILBs, though it has been reported in previous studies that the bottom of the parabolic band (minimum value) appears at ~0.5 eV from the Fermi level. in the present measurement, the bottom of the ILB and the top of the valence band of bulk SiC overlapped in the present measurement, so it was difficult to determine the existence of ILB.

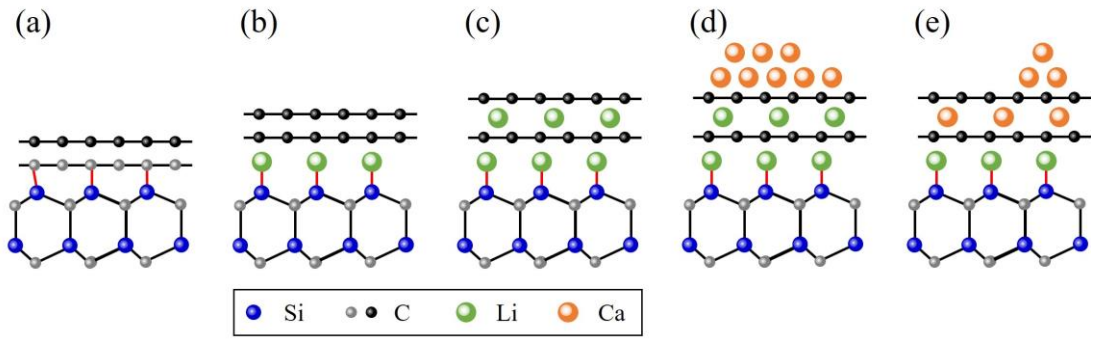

Figure 3, Stacking structure model of Ca-intercalated graphene during the fabrication process. (a) Pristine monolayer graphene on SiC substrate. The upper graphene layer (black) is freestanding monolayer graphene, and the lower layer (gray) is a buffer layer bonded to the SiC substrate. (b) Li deposition terminates the SiC surface with Li atoms to form freestanding bilayer graphene. (c) (b) is further Li-deposited, and Li atoms are intercalated between graphene layers. (d) Ca layer is grown on the top surface by Ca deposition. (e) Ca atoms are intercalated by annealing.

7. Discussion

The stacking structure model of the sample preparation process of Ca-intercalated graphene considered from the above results is shown in Figure 3. First, Li deposition transforms the monolayer graphene (Fig. 3 (a)) into freestanding bilayer graphene (Fig. 3 (b)), and then Li atoms are intercalated between the bilayer graphene (Fig. 3 (c)). The Ca is not intercalated into the interlayer when only deposited (Fig. 3 (d)), but is intercalated into the graphene only after annealing at high temperature (Fig. 3 (e)). Therefore, it is clear that two-dimensional superconductivity is observed in the structure where the SiC surface is terminated with Li and Ca is intercalated between the freestanding bilayer graphene layers.

The origin of the superconductivity is most likely the ILB or π^* band rather than the flat band of vHs, and the possibility of a mixture of the two is also suggested by the transport measurements. The above idea is also supported by the fact that the ARPES results expected vHs-induced superconductivity in Li-intercalated graphene, but no superconducting transition was observed in the transport measurements.

8. Conclusion

In this study, we have conducted a systematic investigation of superconducting graphene interlayers using both transport and ARPES measurement approaches. As a result, we have clarified the stacking

structure model of the sample in which superconductivity is observed, and revealed that the superconductivity is in freestanding bilayer graphene with Ca atoms in between; the lower C layer is released from the SiC substrate due to the SiC surface termination by Li atoms. The superconductivity is most likely due to the ILB or π^* band. By changing the incident photon energy in ARPES and obtaining ARPES images where the 3D bulk band does not overlap with the ILB, it is hoped that we will be able to confirm whether the superconductivity is induced by ILBs like Ca-intercalated bilayer graphene as in previous studies or not. In addition, by measuring the structure and transport properties of a sample with a reduced number of layers and only a buffer layer grown on a SiC substrate (0-layer graphene covered from the buffer layer), we aim to verify the stacking model assumed in this study and construct a more accurate model.

9. Acknowledgement

We would like to express our gratitude to our advisors, Professor Shuji Hasegawa of the Department of Physics, The University of Tokyo, and Associate Professor Toru Hirahara of Department of Physics, Tokyo Institute of Technology, for their great support and guidance in carrying out this research. We would like to express our gratitude to Assistant Professor Ryota Akiyama of Hasegawa Laboratory, University of Tokyo, Assistant Professor Satoru Ichinokura of Hirahara Laboratory, Tokyo Institute of Technology, and Dr. Yukihiro Endo, a graduate of Hasegawa Laboratory, University of Tokyo, for their guidance and cooperation in this research. We would also like to thank Haruko Toyama's associate advisor in the MERIT program, Professor Yoshihiro Iwasa, for his kind permission to propose this research. Finally, we would like to express our sincere gratitude to the MERIT program for giving us the opportunity to conduct this research.

10. Reference

1. S. Ichinokura et al., Acs Nano 10, 2761 (2016).
2. K. Kanetani et al., Proceedings of the National Academy of Sciences 109, 19610 (2012).
3. B. Ludbrook et al., Proceedings of the National Academy of Sciences 112, 11795 (2015).
4. A. M. Black-Schaffer and C. Honerkamp, Journal of Physics: Condensed Matter 26, 423201 (2014).
5. J. L. McChesney et al., Physical review letters 104, 136803 (2010).
6. Y. Endo et al., Carbon 157 857-862 (2020).
7. Y Endo, Doctoral Dissertation, Department of Physics, Graduate School of Science, The University of Tokyo (2020).
8. M. Kusunoki et al., Applied Physics Letters 77, 531 (2000).
9. A. Larkin and A. Varlamov, Theory of Fluctuations in Superconductors (Clarendon Press, Oxford, U.K., 2005).

10. R. S. Thompson, Phys. Rev. B 1, 327 (1970).
11. V. Ginzburg, Physics Letters 13, 101 (1964).